ELSEVIER

www.elsevier.nl/locate/carres

Carbohydrate Research 324 (2000) 242–254

CARBOHYDRATE RESEARCH

Conformational studies of the glycopeptide Ac-Tyr-[$Man_5GlcNAc$-β-(1 → 4)GlcNAc-β-(1 → N^{δ})]-Asn-Leu-Thr-Ser-OBz and the constituent peptide and oligosaccharide

David Bailey [a], David V. Renouf [a], David G. Large [b], Christopher D. Warren [c], Elizabeth F. Hounsell [a,*]

[a] *School of Biological and Chemical Sciences, Birkbeck University of London, Gordon House, 29 Gordon Square, London WC1H 0PP, UK*

[b] *School of Chemistry & Pharmacy, Liverpool John Moores University, Byrom Street, Liverpool L3 3AF, UK*

[c] *Department of Biomedical Sciences, Shriver Center for Mental Retardation, Waltham, MA 02452, USA*

Received 10 June 1999; accepted 3 September 1999

Abstract

Glycopeptides of desired structure can be conveniently prepared by the coupling of reducing oligosaccharides to aspartic acid of peptides via their glycosylamines formed in the presence of saturated aqueous ammonium hydrogen carbonate. The resulting oligosaccharide chains are N-linked to asparagine as in natural glycoproteins, allowing different peptide oligosaccharide combinations to be analysed for conformational effects. In the present paper, a pentapeptide of ovalbumin was coupled to $Man_5GlcNAc_2$ oligosaccharide and the glycopeptide and the two parent compounds compared by NMR ROESY experiments and molecular dynamics simulations. Despite the small size of the peptide, conformational effects were observed suggestive of the oligosaccharide stabilising the peptide in solution and of the peptide influencing oligosaccharide conformation. These effects are relevant to the function of glycosylation and the enzymic processing of oligosaccharide chains.

Keywords: ROESY; Conformation; Glycopeptides; N-glycosylation

1. Introduction

Despite the growing awareness of the role of protein glycosylation in specific recognition and cell signalling, less is known about the effect of oligosaccharides on protein conformation and how peptide affects glycan structure. We are attempting to shed light on these effects by detailed NMR spectroscopy studies of chemically synthesised glycopeptides and glycosylated immunoglobulin light chains from primary systemic amyloidosis patients [1]. It is now widely accepted that specific peptide sequences distant from the glycosylation site regulate the interaction with the glycosyltransferases, which catalyse the biosynthesis of specific recognition motifs. This is further influenced by hormonal or cytokine regulation and cell-culture conditions [2]. However, the mechanism for the decision to

* Corresponding author. Tel.: +44-207-679-7468; fax: +44-207-679-7464.

E-mail address: e.hounsell@bbk.ac.uk (E.F. Hounsell)

0008-6215/00/$ - see front matter
PII: S0008-6215(99)00247-5

have a high mannose, hybrid or complex chain at a particular consensus N-glycosylation site is not known. There are now many examples of specific glycoforms at specific sites, the most remarkable perhaps being that reported by Dahms and Hart [3] of quaternary effects of the different α subunits of Mac-1 and LFA-1 influencing the different site-specific glycosylation of the identical (by amino acid sequence) β subunits.

From what we know so far about N-linked glycosylation, oligosaccharides are transferred from a preformed dolichol-glycan to nascent polypeptide chains via the enzyme oligosaccharyl transferase, which is part of the ribosomal enzyme complex [4,5]. Ronin et al. [6] could find no evidence for substrate specificity of the transferase isolated from the thyroid gland beyond the consensus sequence Asn.Xaa.Ser/Thr, where the oligosaccharide chain transferred to the acetamido group of Asn and Xaa can be any amino acid except Pro [7]. However, there is growing evidence that acceptor recognition of the glycosyltransferases, which are involved in downstream processing of N-glycosylation, is affected by amino acid sequences distal to the glycosylation-protein attachment site [8,9]. There is also a growing X-ray crystallographic database of the types of peptide structural motifs that support glycosylation. This can be accessed from the Brookhaven protein data base (PDB) [10–12] and shows occupied N-glycosylation consensus sites in all four main protein structural motifs. Several models have been proposed to describe the mechanism of the transfer interaction [13–15], but these have so far not explained how the protein sequence dictates the type of glycosylation, i.e., why certain peptide sequences containing the consensus sequon are not glycosylated and how the glycosylation affects the protein conformation. Comparison of the solution conformation of synthesised glycopeptides having different peptide sequences would add information to the data base of crystallised glycoproteins, the most recent study of which [12] has shown quite restricted dihedral angles for oligosaccharides in different glycoproteins.

In the present studies we have investigated a glycopeptide having the $Man_5GlcNAc_2$ oligosaccharide coupled to the amino acid sequence taken from around the glycosylated Asn 298 (α_1-antitrypsin numbering) in the serine proteinase inhibitor hen egg ovalbumin, for which X-ray crystallographic coordinate data are available [16,17]. The $Man_5GlcNAc_2$ structure stands at a crossroads in biosynthesis as it is the acceptor for the first glucosaminyltransferase in the Golgi leading to complex and hybrid chains. The peptide, glycopeptide and oligosaccharide have been characterised by homonuclear ^1H NMR spectroscopy experiments, 2D ^1H–^1H DQFCOSY, ^1H–^1H TOCSY and ^1H–^1H ROESY, and distinct differences in chemical shifts and ROEs found suggest oligosaccharide conformational differences, which may in turn affect oligosaccharide processing. In addition, computer graphics molecular modelling and molecular dynamics simulations have shown that even with only a small number of amino acids present, the peptide is significantly stabilised by the presence of glycosylation.

2. Experimental

Glycopeptide synthesis.—The oligosaccharide of empirical formula $Man_5GlcNAc_2$ was isolated as a catabolic product from the urine of swainsonine-treated sheep and purified by gel filtration and normal phase high-performance liquid chromatography (HPLC) on an amine bonded silica column with water–acetonitrile as solvent. The identity was confirmed by the NMR spectroscopy. The glycosylamine of the oligosaccharide was prepared in one step by the method originally proposed by Likhosherstov et al. [18] i.e., by reaction with satd aq ammonium hydrogen carbonate followed by evaporation and repeated evaporation from water. The peptide was synthesised by solution chemistry, stepwise from the C-terminus using Fmoc pentafluorophenyl esters. The glycopeptide link was constructed in a convergent fashion [19] by condensing the heptasaccharide glycosylamine with the hydroxybenzotriazole (HBT) ester of the protected peptide Fmoc-Tyr-Asp(β-COOH)-Leu-Thr-Ser-OBz, formed in situ with HBT-2-(1H-benzotriazol-1-yl)-

1,1,3,3,-tetramethyluronium hexafluorophosphate. The yield of pure glycopeptide, Ac-Tyr-(Man_5GlcNAc-GlcNAc-β-(1→N^{δ}))Asn-Leu-Thr-Ser-OBz, was 54%.

NMR spectroscopy.—The heptasaccharide and glycopeptide (2.5 mg of each) and the peptide (1.5 mg) were dissolved in distilled degassed water and the sample volume adjusted to 600 μL by addition of D_2O (99.96%) to give a 90% H_2O–10% D_2O mixture. ^1H–^1H TOCSY [20–22], ^1H–^1H DQF-COSY [23], ^1H–^1H ROESY [24,25] and ^1H 1D spectra were obtained using Varian 500 Unity Plus and Varian 600 Unity NMR spectrometers. Solvent suppression was carried out by presaturation [26] or by WATERGATE [27]. The 2D ROESY spectra were acquired using a pulsed-field-gradient variant of the ROESY experiment (hypercomplex method [28]) at 298 K with a mixing time of 300 ms.

Molecular modelling.—The oligosaccharides were constructed from a set of monosaccharides added to the software modelling package Insight II (v. 97.0; Molecular Simulations Inc.) with potential types and charges assigned manually in the AMBER forcefield as described previously [29]. The peptide from the X-ray coordinates for ovalbumin from the PDB (Brookhaven) file PDB1OVA was excised from the protein, the oligosaccharide amide removed and the blocking groups added to mimic the missing protein [30]. The heptasaccharide was added to this protected peptide using the X-ray coordinate geometry around the glycosylation bond. The reducing heptasaccharide, the peptide and glycopeptide were each randomised to 50 different starting geometries for simulated annealing and minimisation using a distance-dependent dielectric term to simulate a water environment and the distances for which inter-residue ROEs were found were restrained to 4.5 Å or less. Minimisation was to a maximum derivative 0.001 kcal/Å. For annealing by molecular dynamics a harmonic potential for bond energies and the leap-frog algorithm were used in the

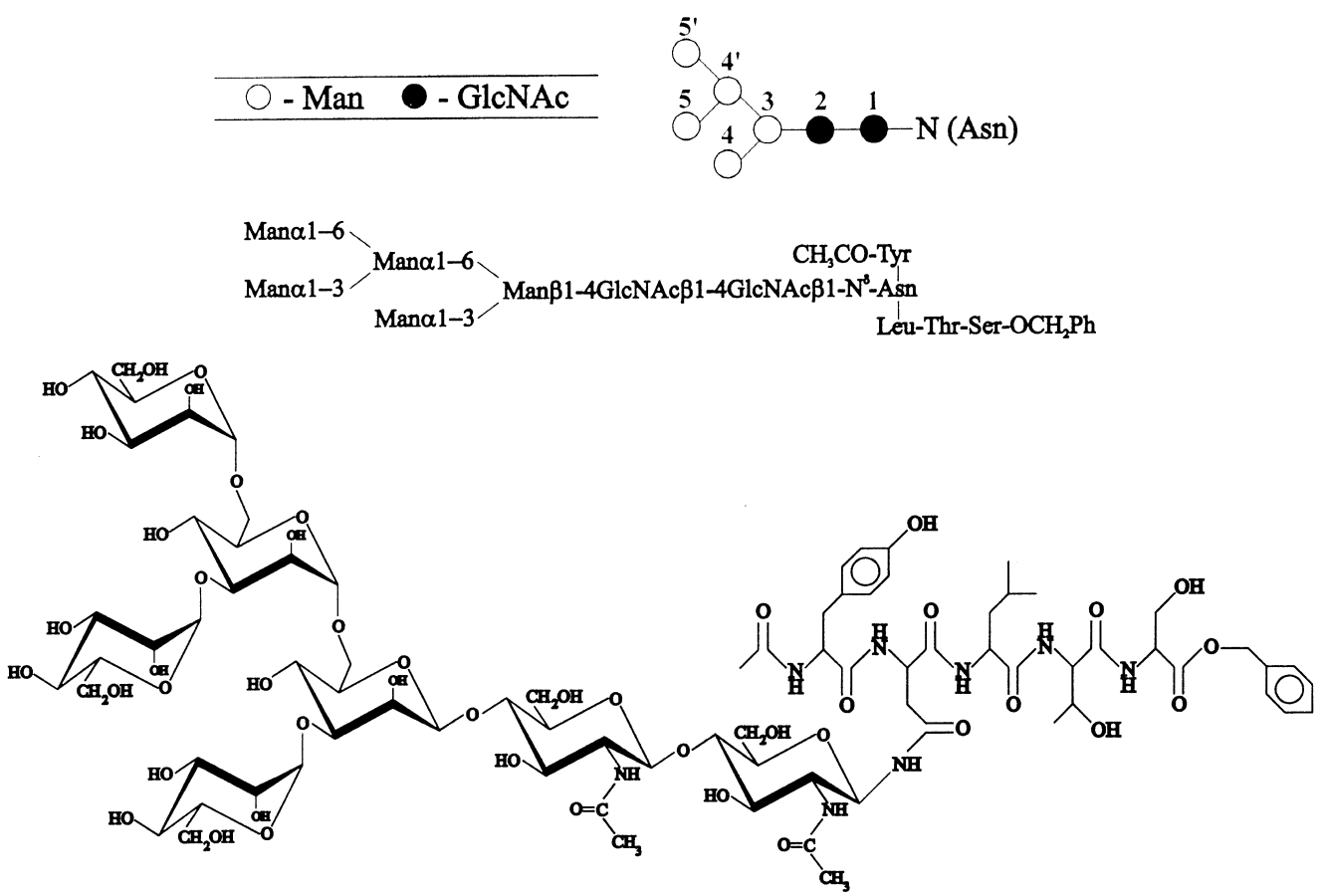

Fig. 1. Structural schematic of the glycopeptide.

DISCOVER program (MSI). The structures were equilibrated for 1 ps at 1000 K (1 fs steps) and held at that temperature for 50 ps of molecular dynamics before annealing with 2 ps intervals through a cooling phase, where the temperature was decreased in 20° steps to 20 K. After annealing, the structure was minimised. Sugar ring geometries were restrained (1 kcal/Å) at temperatures above 300 K. Structures with high relative energies (e.g., for the glycopeptide >800 where the normal range was -5.6 to 20.8) were rejected as they demonstrated impossible conformations with bonds passing through aromatic ring structures. Of the remaining conformations, 30 were selected at random and their dihedral angles measured and compared with those of Imberty et al. [31]. The most populated oligosaccharide dihedral ranges agreed with the published values, which were then used to compare molecular dynamic simulations for the peptide and glycopeptide carried out in a 30 Å water box (in Insight II) under the same molecular dynamics conditions as above. An averaged structure of the 30 conformations in vacuo was produced by the module Decipher in Insight. This was then minimised and backbone RMSD comparisons made with the 30 pre-averaged conformations and with the starting geometry before molecular dynamics.

3. Results

The effects of glycosylation on peptide conformation.—A near-complete chemical shift assignment has been made for the glycopeptide (Fig. 1) and constituent oligosaccharide and peptide as described below. This was used to interpret the ROE data for the first two molecules, which were inputted as constraints in the molecular modelling. For the molecular models starting from 30 randomised geometries, using a distance-dependent dielectric, the RMSD of each compared with the averaged structure was as follows: reducing heptasaccharide 3.45–5.82, Av 4.92; peptide 1.41–2.45, Av 1.93; glycopeptide 1.26–3.00, Av 2.10. The RMSD of the glycopeptide compared with the starting X-ray peptide was 1.96. Comparison of the RMSD of the final glycopeptide structure in water with that of the averaged structure in vacuo (distance-dependent dielectric) was 2.33. These data for the peptide and glycopeptide are consistent with high-resolution structures compared with the free oligosaccharide. As summarised in Table 1, the striking aspect of the molecular modeling was the apparent stabilisation of the peptide by glycosylation. Thus, compared with the distance geometry data for the

Table 1
Comparison of the distance geometry of the peptide Ac-Tyr-Asp-Leu-Thr-Ser-OBz and the glycopeptide (Gp), with Asp replaced by heptasaccharide-Asn, from the X-ray coordinate data and after molecular dynamics (MD) in water or the average (Av) from randomised starting geometries with or without ROE restraints (R) on the oligosaccharides

Interaction	Gp	Peptide		Gp		
	Distance (X-ray)	Distance by MD		Distance by MD		
		Water	Av	Water	Av+R	Av−R
Tyr N–H/Ac CH_3 [a]	3.87	2.89	3.58	3.87	3.86	3.88
Tyr N–H/Tyr Cα–H	2.93	2.17	2.18	2.98	2.97	2.87
Asp N–H/Tyr Cα–H	2.37	2.86	3.62	2.75	2.29	3.57
Asp or Asn N–H/Asp or Asn Cα–H	2.88	2.85	2.16	2.89	2.99	2.82
Leu N–H/Asp or Asn Cα–H	2.13	3.54	2.16	2.30	2.30	2.71
Leu N–H/Leu Cα–H	2.94	2.26	2.80	2.95	2.22	2.23
Thr N–H/Leu Cα–H	3.54	2.61	4.06	2.63	3.59	2.77
Thr N–H/Thr Cα–H	2.84	2.66	2.82	2.97	2.92	2.21
Ser N–H/Thr Cα	2.88	3.68	3.51	2.50	2.23	2.65
Thr Cβ–H	3.63			4.00		
Ser N–H/Ser Cα–H	2.83	2.72	2.18	2.77	2.90	2.91

[a] Averaged valued over CH_3.

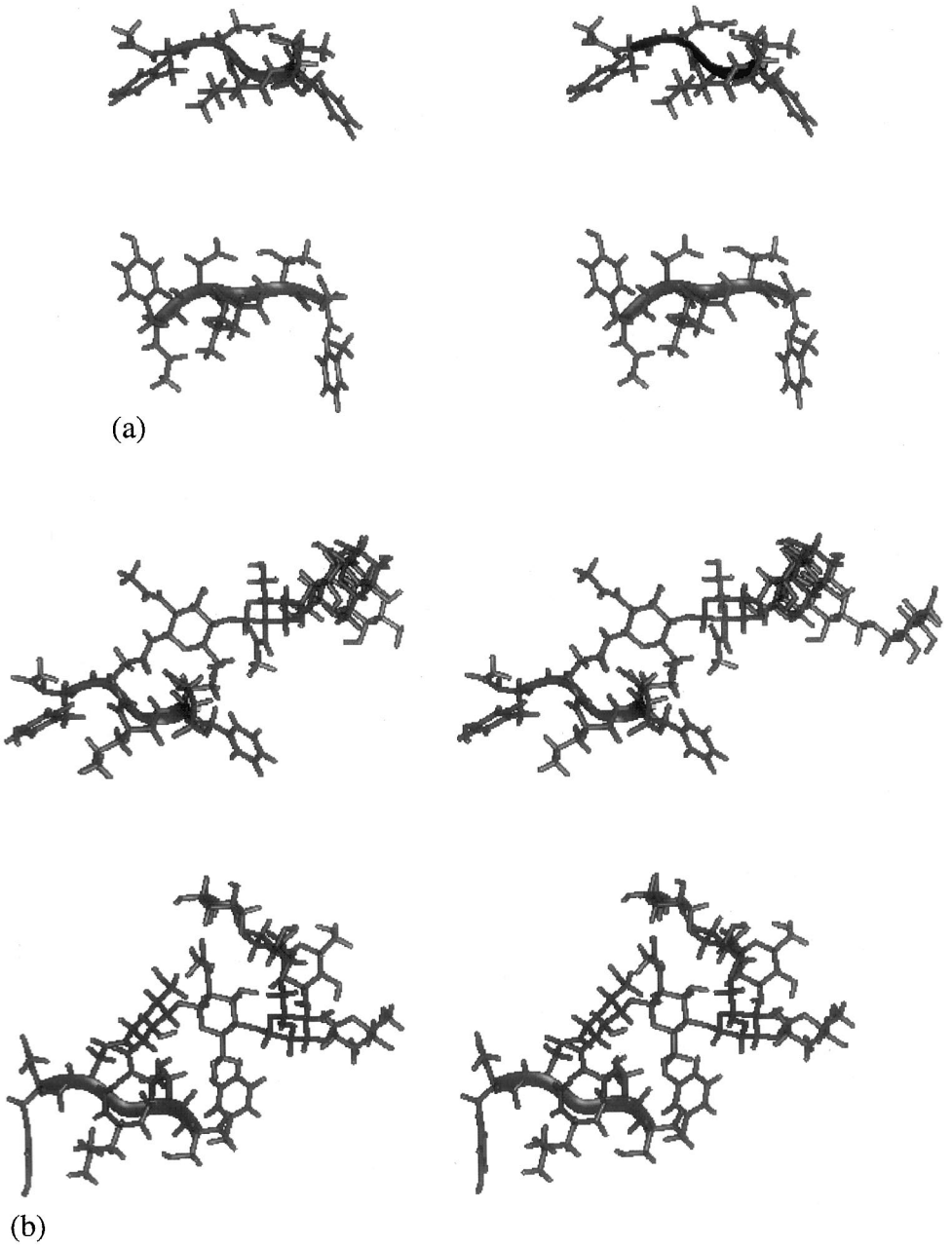

Fig. 2. Stereo diagrams of (a) the peptide, and (b) the glycopeptide after molecular dynamics in a water box with the starting (top) and finishing (bottom) geometries. The amino terminus of the peptide is on the left as depicted in Fig. 1.

peptide, those for the glycopeptide after molecular dynamics in water or in vacuo with added ROE constraints are very similar to the starting X-ray structure. Fig. 2 depicts this for the molecular dynamics carried out in water.

Table 2 gives the complete chemical shift assignments for amino acids of the peptide and glycopeptide. There are significant differences in chemical shifts ($>\Delta\delta$ 0.03) for Tyr H–Cα and Ser H–N and of the coupling constant of Tyr H–N. Fig. 3 gives the ROESY spectra of the H–N region of the peptide and glycopeptide, showing the increased Ser ROEs in the peptide compared with the glycopeptide and inter alia the H–N chemical shift. The Tyr H–N is clearly seen in both spectra from which the coupling constant was calculated. The signals could be readily assigned for the five amino acids in the glycopeptide from

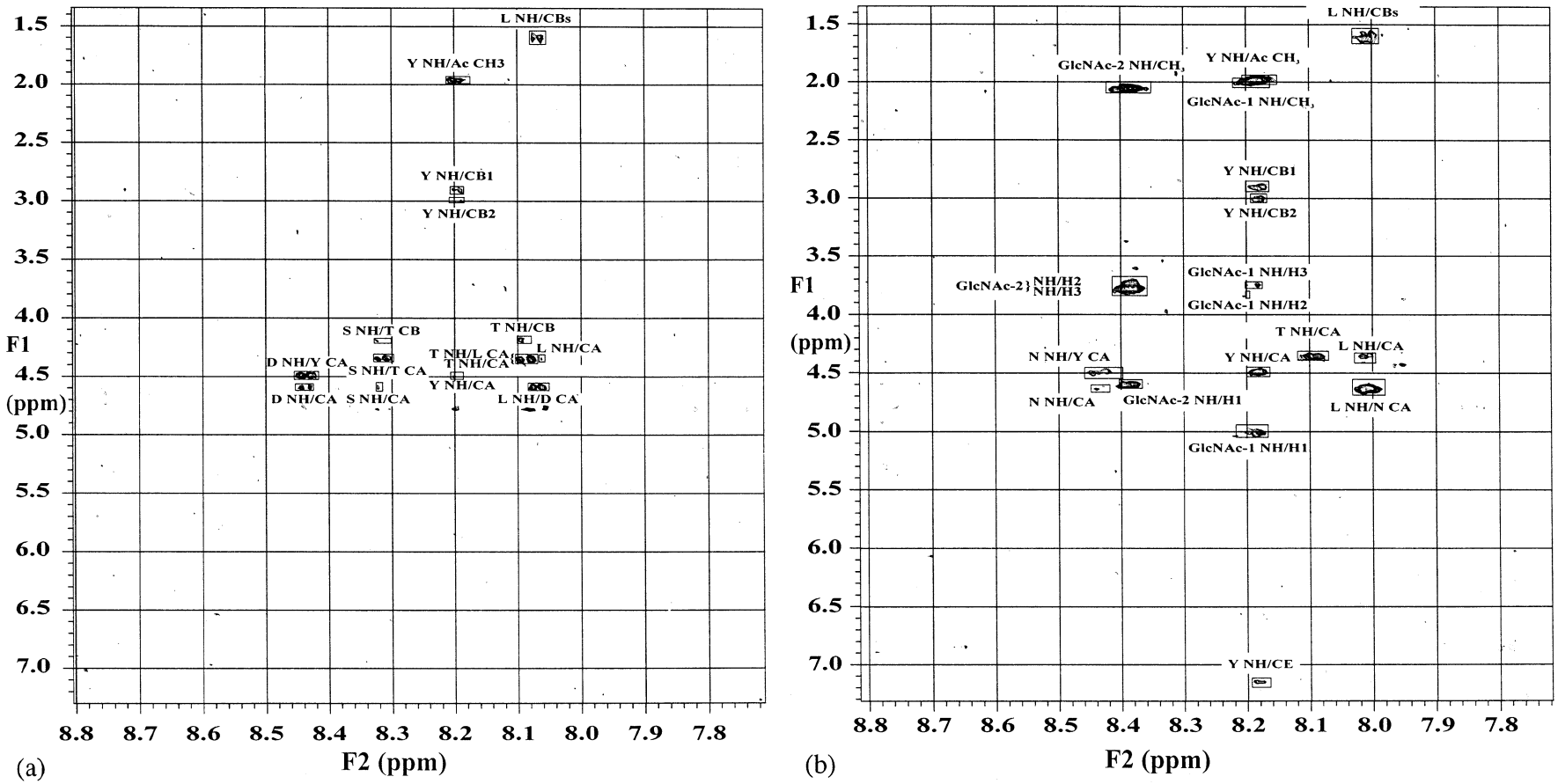

Fig. 3. ROESY spectra of (a) the peptide, and (b) the glycopeptide, for comparison of the cross-peak intensities. CB and CA refer to the protons at Cβ and Cα.

TOCSY spectra and a 1D ^{1}H spectrum. The N-terminal Tyr residue has characteristic resonances in the aromatic region of the 1D ^{1}H NMR spectrum, with the H-C$^{\delta}$s and H-C$^{\varepsilon}$s forming two doublets at 7.139 and 6.839 ppm, respectively. The H-C$^{\delta}$ was assigned the downfield shift due to the correlation with H–C$^{\beta}$ Tyr. A H–N/H–C$^{\alpha}$ cross-peak in the TOCSY spectrum was visible at 8.181/4.479 ppm and H–C$^{\alpha}$/C$^{\beta}$, H-C$^{\beta1}$/C$^{\beta2}$ cross-peaks at 2.892/2.998 ppm to H–C$^{\varepsilon}$. The Asn residue shows H–C$^{\alpha}$/C$^{\beta}$ cross-peaks (4.626/2.631 ppm), H–C$^{\beta1}$/C$^{\beta2}$ (2.631/2.802 ppm) and H$^{N\delta}$/GlcNAc H-1 (8.555/5.010 ppm) together with

Table 2
The ^{1}H NMR chemical shifts (δ from acetone at 2.225 ppm at 25 °C) and coupling constants J (Hz) for the peptide Ac-Tyr-Asp-Leu-Thr-Ser-OBz and glycopeptide (Gp) with Asp replaced by heptasaccharide-Asn

	Peptide		Gp	
	ppm	*J*	ppm	*J*
Tyr				
H–Cα	4.515		4.479	
H–Cβ1	2.912	14.3, 7.9	2.892	14.1, 8.3
H–Cβ2	7.135	13.8, 6.8	2.998	13.8, 6.6
H–Cδ	6.841	8.7	7.139	8.7
H–Cε	3.005	8.7	6.839	8.7
H–N	8.205	7.1	8.181	5.9
Asp/Asn				
H–Cα	4.580		4.626	
H–Cβ1	2.675	17.1, 7.1	2.631	16.4, 6.3
H–Cβ2	2.847	16.7, 7.1	2.802	16.4, 6.3
H–Nδ			8.555	
H–N	8.444	7.9	8.427	
Leu				
H–Cα	4.352		4.346	
H–Cβ1/β2	1.60/1.64		1.60/1.64	
H–C$^{\gamma}$	1.584		1.568	
H–Cδ1	0.857	6.1	0.851	6.1
H–Cδ2	0.922	6.9	0.917	6.1
H–N	8.070	6.4	8.011	6.6
Thr				
H–Cα	4.353	8.4	4.350	
H–Cβ	4.196	4.1	4.179	
H–C$^{\gamma}$	1.159	6.5	1.159	6.5
H–N	8.089	7.9	8.092	7.5
Ser				
H–Cα	4.602		4.600	
H–Cβ1	3.986	11.9, 4.8	3.983	unresolved
H–Cβ2	3.885	11,9, 4.8	3.885	unresolved
H–N	8.322	7.9	8.388	unresolved

Table 3
The ^{1}H NMR chemical shifts (δ from acetone at 2.225 ppm at 25 °C) of the heptasaccharide $Man_5GlcNAc_2$ free in solution (oligo) and coupled to peptide (Gp)

	Oligo		Gp
	α	β	
GlcNAc-1			
H-1	5.191	4.696	5.003
H-2	3.874	3.693	3.830
H-3	3.88	3.688	3.737
H-4	3.625	3.624	3.633
H-5	3.879	3.507	3.518
H-6	3.791	3.834	3.797
H-6	3.673	3.668	3.895
NAc	2.039	2.039	1.991
	8.165	8.206	8.196
GlcNAc-2			
H-1	4.594	4.584	4.588
H-2	3.789		3.775
H-3	3.766		3.77
H-4	3.739		3.720
H-5	3.605		3.596
H-6	3.879		3.876
H-6	n.d. [a]		n.d. [a]
NAc	2.065		2.050
	8.409		8.385
Man-3			
H-1	4.771		4.774
H-2	4.253		4.252
H-3	3.756		3.758
H-4	3.785		3.77
H-5	3.636		3.634
H-6	3.951		3.949
H-6	n.d. [a]		3.768
Man-4			
H-1	5.095		5.093
H-2	4.080		4.084
H-3	3.893		3.894
H-4	3.803		3.813
H-5	3.636		3.638
H-6	3.917		3.917
H-6	n.d. [a]		3.744
Man-4′			
H-1	4.870		4.869
H-2	4.148		4.145
H-3	3.920		3.918
H-4	3.880		3.881
H-5	3.849		3.848
H-6	3.987		3.977
H-6	3.738		3.738
Man-5			
H-1	5.091		5.089
H-2	4.068		4.068
H-3	3.891		3.888
H-4	3.771		3.772
H-5	3.674		3.675
H-6	n.d. [a]		n.d. [a]
H-6	n.d. [a]		n.d. [a]
Man-5′			
H-1	4.906		4.905
H-2	3.983		3.990
H-3	3.842		3.840
H-4	3.774		3.739
H-5	3.656		3.677
H-6	3.897		3.895
H-6	n.d. [a]		n.d. [a]

[a] n.d., not determined.

a weak H–N/C–C^{α} correlation (8.427/4.626 ppm). A DQF-COSY spectrum (not shown) gave the full coupling network of the Thr residue of the glycopeptide and the two H-C^{δ}s of Leu (0.851/0.917 ppm) to the H-C^{γ} (1.568 ppm), which is in turn coupled to the two H-C^{β}s (1.60 and 1.64 ppm). The Leu H-C^{β} shows coupling to the H–C^{α} (4.346 ppm) with the final coupling being the H–N/H–C^{α} cross-peak (H-N 8.011 ppm). The DQF-COSY experiment also revealed the Asn H–N^{δ}/GlcNAc H-1 cross-peak and the H–N/H–C^{α} cross-peaks. H–N/H–C^{α}, H–N/H–C^{β} and H–N/H–C^{γ}, H–N/H–C^{δ} couplings were assigned from the TOCSY experiment.

The effect of peptide on oligosaccharide conformations.—The chemical shifts for the oligosaccharide portion of the glycopeptide are shown in Table 3. Compared with the chemical shifts of the free oligosaccharide (β), there were large differences for the H-1 of GlcNAc-1 and smaller differences for the H-4 and the CH_3 resonance of GlcNAc-2 ($>\Delta\delta$ 0.15) and the H-4 ($>\Delta\delta$ 0.03) and H-5 ($>\Delta\delta$ 0.02) of Man-5′. Fig. 4 shows the H-1 track for GlcNAcβ1-(Asn). The signals for H-3 and H-4 were assigned (Table 3) by comparison with the literature (e.g., [32]). Although this assignment is the most likely one from comparison of the chemical shifts for the oligosaccharide, the resulting ROE in the glycopeptide from H-1/H-4 rather than H-3, as shown in Table 4, is most unlikely and is more likely due to Hartmann–Hahn transfer from H-5, with H-1/H-3 ROE missing due to transfer with H-2 (which has the opposite sign, Fig. 4). In addition to distinct differences in chemical shift at C-2, the ROESY spectra (Figs. 3(b) and 5) revealed NH/CH_3 cross-peaks, which allowed assignment of the NHCO–CH_3 singlets in the 1D spectrum (one at 8.193/1.991 ppm, the other at 8.385/2.050 ppm) and the GlcNAc acetyl H-N/H-2 coupling. These spectra show distinct differences in the intra-ring ROEs for the oligosaccharide and glycopeptide with respect to the orientation of the NHCO–CH_3 group (Table 4). Thus, Fig. 5 shows a stronger H-N/H-2 ROE than that of H-N/H-1 or H-N/H-3 for the GlcNAcβ of the reducing GlcNAc, whereas Fig. 3(b) shows a strong H-N/H-1 ROE (5.0–8.2 ppm) and weaker ROEs for H-N/H-2 (3.7–8.2 ppm) and H-N/H-3 (3.75–8.2 ppm) in the glycopeptide. The modelling in Fig. 2(b) shows, in the final conformation of the glycopeptide, the N-acetamido group of GlcNAc-1 in close prox-

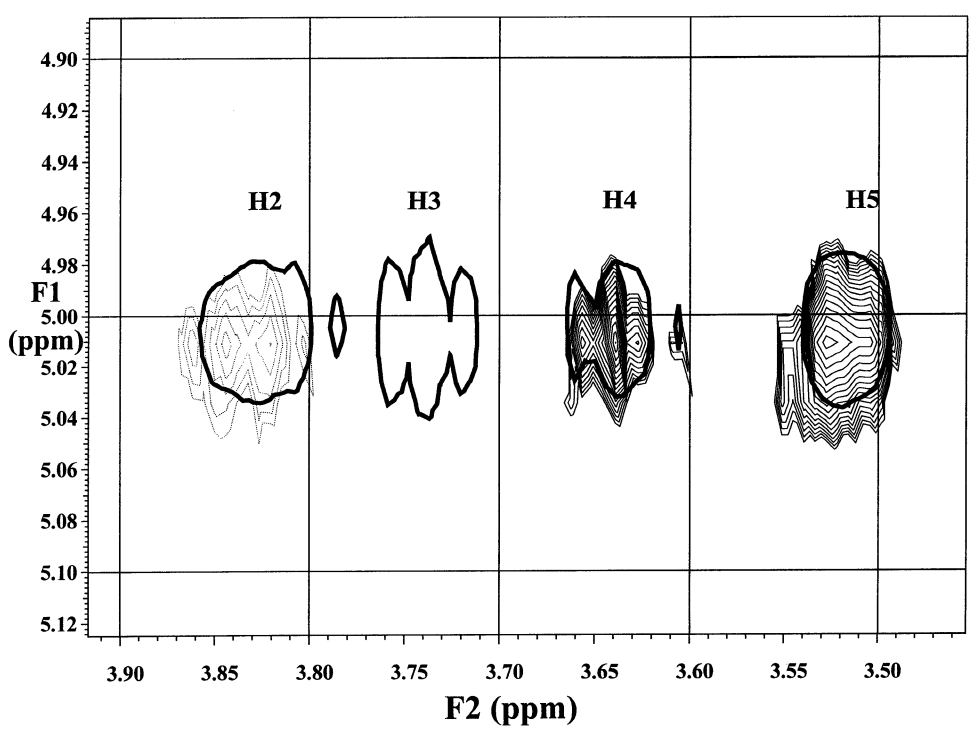

Fig. 4. The H-1 track for GlcNAcβ1-(Asn) showing the outline of the TOCSY cross-peaks in bold with the superposed ROE contours and as the dotted line, a TOCSY effect (opposite sign).

imity to the peptide, which could account for the distinct differences in ROE intensities around H-2 in this residue.

Fig. 6 shows a section of the TOCSY spectrum of the daughter oligosaccharide from which the rest of the signals were assigned. Although the residual water signal after presaturation (see Section 4) hides the Man-β-(1→4) H-1 proton signal, the other H-1 signals are all visible. The H-1/H-2 cross-peak for the reducing-end GlcNAcβ was shown at 4.70/3.69 ppm with the α anomer at 5.19/3.87 ppm [33]. The two Man-α-(1→3) and two Man-α-(1→6) residues were readily identified from the H-2 and H-3 cross-peaks at the chemical shifts of H-1, i.e., 5.10, 5.09 ppm for Man-α-(1→3) and 4.87, 4.91 ppm for Man-α-(1→6). Further signals for the Man-α residues were assigned from the cross-peaks at the chemical shifts of H-2 (Fig. 6), including the Man-β-(1→4) H-3 to H-6 signals from the cross-peaks at the chemical shift of H-2 (4.25 ppm). The internal GlcNAc-β-(1→4) residue gave cross-peaks for H-1 to H-6 at the chemical shifts of H-1 of 4.59 and 4.58 ppm (caused by anomerisation from the reducing-end GlcNAc). Alteration of the contour levels allowed the majority of their associated cross-peaks to be assigned (Table 3). Of the coupling constants for GlcNAc-1, besides H-1, that could be unambiguously assigned, $J_{5,6}$, normally around 6 Hz as found here for the oligosaccharides, was nearer 4 Hz in the glycopeptide. For the mannoses, in addition to the expected ROEs, there were stronger ROEs in the glycopeptide compared with the oligosaccharide (Table 4): (i) across the linkage Man-α-(1→3)-Man-β from H-1 of Man-α to H-5 of Man-β; (ii) across the linkage Man-α-(1→6)-Man-β from H-2 of Man-α to H-6 of Man-β; (iii) across the linkage Man-α-(1→6)-Man-α-(1→6) from H-2 of Man-5′ to H-6 of Man-4′ (the Man-5′ also shows significant differences in chemical shift between the peptide and glycopeptide (Table 3).

Table 4
Comparison of the normalised ROE intensities for the oligosaccharide (Oligo) and glycopeptide (Gp)

ROE [c]	Oligo	Gp	Comments
GlcNAc-1β			
H-3/H-1	0.5	NP [a]	greater in oligo [b]
H-4/H-1	0.2	0.5	
H-5/H-1	1	1	
H-6/H-5	0.2	0.2	
N-H/H-1	0.04	0.3	greater in Gp
N-H/H-2	0.07	0.02	greater in oligo
N-H/H-3	NP	0.1	greater in Gp
GlcNAc-1α			
H-1/H-2	1		
N–H/CH_3	0.2		
N–H/H-1	0.01		
N–H/H-2	0.3		
GlcNAc-2			
N–H/CH_3	0.3	1	
N–H/H-1	0.1	0.3	
GlcNAc-1/ GlcNAc-2			
1βH-5/H-1	0.2	0.6	
1αH-6/H-1	1		
Man-3/Man-4			
H-2 4/H-5	NP	1	greater in Gp
H-5/H-1	NP	1	greater in Gp
H-2/H-1	1	0.1	
Man-3/Man-4′			
H-4/H-2	1	NP	greater in Oligo
H-6/H-1	0.6	1	
H-6/H-2	NP	0.3	greater in Gp
Man-4′			
H-2/H-1	0.7	0.2	
Man-4′/Man-5			
H-2/H-1	1	1	
H-5/H-1	5	0.2	
H-6/H-1	0.9	0.4	
H-5/H-2	1	TE	
H-6/H-2	NP	1	greater in Gp
Man-5′			
H-2/H-1	0.9	0.4	
H-3/H-2	0.8	TE	

[a] Not present.

[b] See text; TE = TOCSY effect.

[c] Additional cross-peaks definitely present but the cross-peak intensities of which could not be measured due to overlapping contours, i.e.: GlcNAc-1β (Gp) N–H/CH_3; GlcNAc-2 (both Oligo and Gp) N–H/H-2, N–H/H-3, H–5/H-1 and from H-1 to GlcNAc-1β H-4; Man-3 (both Oligo and Gp) H-3/H-2; Man-4 (both Oligo and Gp) H-2/H-1, H-3/H-2 (TE in Gp) and H-1 to Man-3 H-3; Man-4′ H-3/H-2 in Oligo, which has a TE in Gp; Man-5 (both Oligo and Gp) H-2/H-1, H-3/H-2 and H-1 to Man-4′ H-3.

4. Discussion

These studies show the feasibility of an approach for analysing the effects of glycosylation on specific amino acid sequences using NMR spectroscopy and computer graphics.

The results have shown that standard experiments, using the 'presaturation' method of water suppression, have weaker signals from the peptide 'NH' region than with the WATERGATE method of suppression. The latter has enabled all the H–N/H–C^{α}s to be assigned and hence to show distinct differences in the peptide backbone with and without glycosylation. These data, interpreted with respect to the molecular graphics, extend previous work of others showing that the presence of oligosaccharide causes a decrease in the conformational mobility of the peptide backbone [34–40]. The relatively small size of the pilot peptide synthesised in the present study made this all the more surprising. The method can now be used to analyse an array of larger and different peptides with N-linked glycosylation. The NMR data for the oligosaccharide free in solution, in comparison to when linked to a peptide, also suggest that quite small peptides can alter the ensemble of structures sampled by the oligosaccharide [32,41], which has been shown by others both by NMR spectroscopy

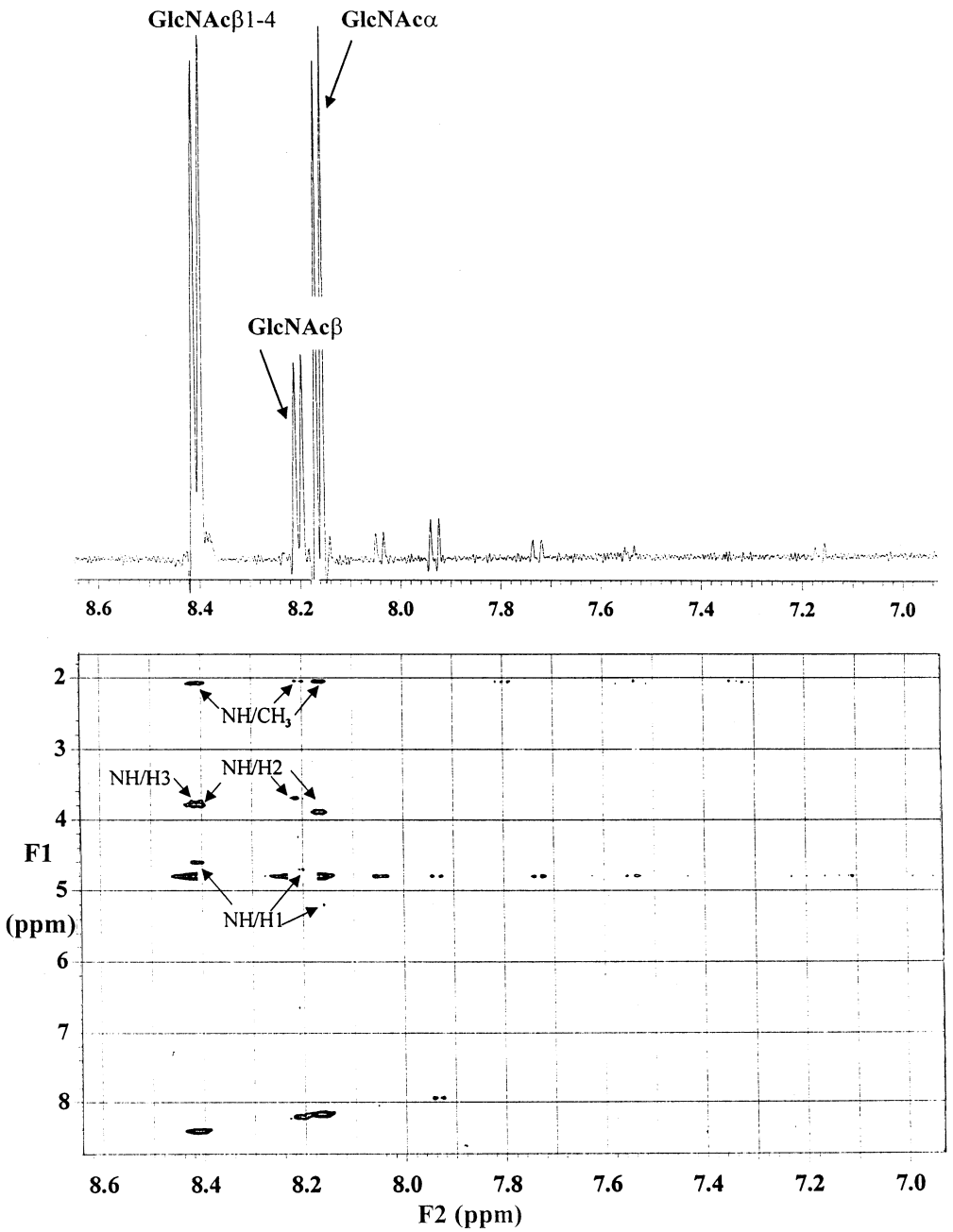

Fig. 5. Superposed 1D ^{1}H and ROESY spectrum showing the H–N signals for the oligosaccharide.

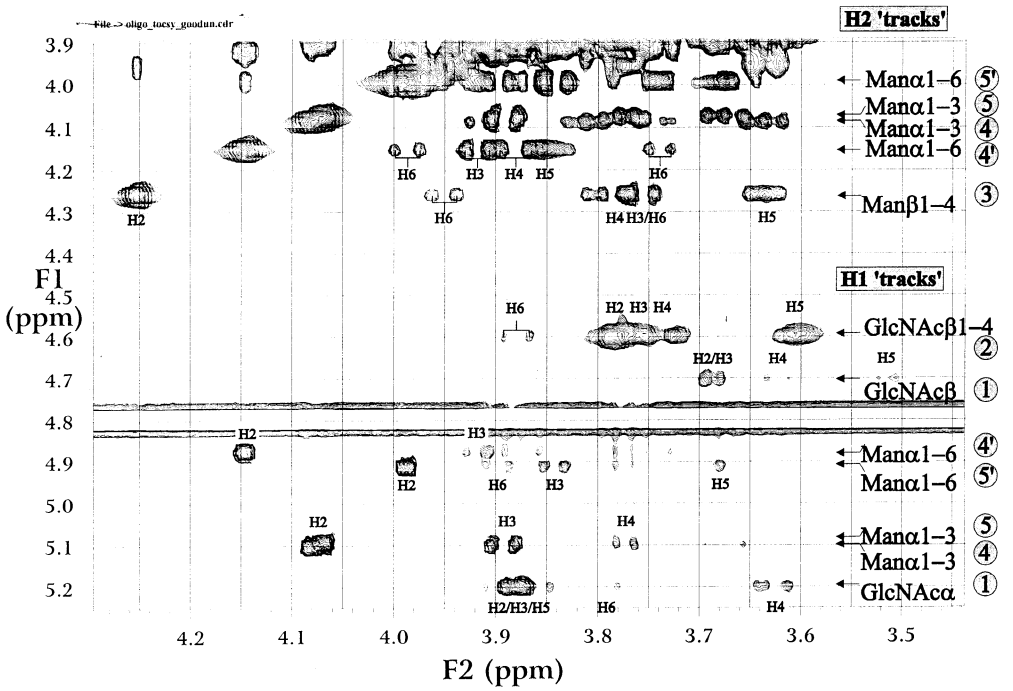

Fig. 6. TOCSY spectrum of the daughter oligosaccharide showing cross-peaks at the chemical shift of H-1 for GlcNAcα/β and Man-α [H1 'tracks'] and H-2 for Man-α and Man-β [H2 'tracks'].

and fluorescence energy transfer (FET) analysis [42,43].

Previously, the synthesis of glycopeptides has been mostly of O-linked chains [44–46] and these have been studied conformationally by NMR experiments [44,47,48]. Syntheses of glycopeptides carrying the N-linked core pentasaccharide have recently been reported [49,50], the latter using glycosylamines for coupling formed after release of reducing oligosaccharides by hydrazinolysis [51]. Extensive NMR studies of oligosaccharides linked to Asn isolated from glycoproteins have been carried out previously [33,52]. The present paper reports a strategy for larger glycopeptides, which will hopefully be amenable to large numbers of peptide analogues where the protecting groups are shown to mimic the rest of the protein in its absence [30,53]. This has allowed detailed NMR analysis of the glycopeptide and constituent oligosaccharide and peptide. Thus, we have been able to show significant differences in the chemical shifts and ROEs between free, reducing oligosaccharide and glycopeptide.

Oligosaccharides are no longer considered to be rigid molecules, but have considerable internal flexibility of the glycosidic linkages [54] and therefore experimental ROESY and NOESY data must contain structural contributions from several oligosaccharide chain conformations and not just a single conformation. An iterative relaxation matrix approach [55], such as that used in CROSREL [56], can allow for this flexibility and be used in conjunction with molecular dynamics simulations starting from random geometries to define the structural characteristics of the different glycosidic linkages, e.g., the internal rotation correlation times [57–60], although these were carried out on small, usually di-, saccharides. Previous studies using NOE analysis have shown the importance of the contribution of the various conformers to the overall structure [54,61–64]. In Taguchi et al. [64], measurement of the rotamer-sensitive mutual spin–spin couplings in the H-5, H-6, H-6′ spin subsystem suggested that the rotamer distributions about the C-5/C-6 bond of the Man-β1 residue would be dependent on oligosaccharide class, i.e., oligomannose, complex, bisected complex or hybrid. Because of the problems in interpreting NOE experiments through spin diffusion, the present study has used ROESY experiments, which have shown additional through-space interactions. Spronk

et al. [60] similarly used combined ROE and molecular dynamics analysis to compare high mannose and hybrid type chains. Thus, in addition to following the stabilisation effects of oligosaccharide on protein and its possible role in protein folding, we have increasing evidence of the conformational preferences of different types of oligosaccharides and glycopeptides, which would be expected to play a part in enzymatic processing and molecular recognition.

Acknowledgements

The authors thank Mrs Gail Evans for her valuable help in preparing this manuscript and the Medical Research Council for funding.

References

[1] L.A. Omtvedt, S. Haavik, E.F. Hounsell, H. Barsett, K. Sletten, *Amyloid*: *Int. J. Exp. Clin. Invest.*, 2 (1995) 150–158.
[2] F.H. Routier, M.J. Davies, K. Bergemann, E.F. Hounsell, *Glycoconjugate J.*, 14 (1997) 201–207.
[3] N.M. Dahms, G.W. Hart, *J. Biol. Chem.*, 261 (1986) 13186–13196.
[4] C. Abeijon, C.B. Hirschberg, *TIBS*, 17 (1992) 32–36.
[5] D.J. Kelleher, G. Kreibich, R. Gilmore, *Cell*, 69 (1992) 55–65.
[6] C. Ronin, C. Granier, C. Caseti, S. Bouchilloux, J. van Rietschoten, *Eur. J. Biochem.*, 118 (1981) 159–164.
[7] Y. Gavel, G. von Heijne, *Prot. Eng.*, 3 (1990) 433–442.
[8] J.U. Baenziger, *FASEB J.*, 8 (1994) 1019–1025.
[9] M.H. Chiu, T. Tamura, M.S. Wadhwa, K.G. Rice, *J. Biol. Chem.*, 269 (1994) 16195–16202.
[10] F.C. Bernstein, T.F. Koetzle, G.J. Williams Jr., E.F. Meyer, M.D. Brice, *J. Mol. Biol.*, 80 (1977) 319–324.
[11] A. Imberty, S. Pérez, *Prot. Eng.*, 8 (1995) 699–709.
[12] A.J. Petrescu, S.M. Petrescu, R.A. Dwek, M.R. Wormald, *Glycobiology*, 9 (1999) 343–352.
[13] A.Y. Avanov, *Molekulyarnaya Biologya*, 25 (1991) 293–308.
[14] I. Meynial-Salles, D. Combes, *J. Biotech.*, 46 (1996) 1–14.
[15] S.E. O'Connor, B. Imperiali, *Chem. Biol.*, 3 (1996) 803–812.
[16] P.E. Stein, A.G.W. Leslie, J.T. Finch, W.G. Turnell, P.J. McLaughlin, R.W. Carrell, *Nature*, 347 (1990) 99–102.
[17] P.E. Stein, A.G.W. Leslie, J.T. Finch, R.W. Carrell, *J. Mol. Biol.*, 221 (1991) 941–959.
[18] L.M. Likhosherstov, O.S. Novikova, V.A. Derevitskaja, N.K. Kochetkov, *Carbohydr. Res.*, 146 (1986) C1–C5.
[19] S.I. Anisfeld, P.T. Lansbury Jr., *J. Org. Chem.*, 55 (1990) 5560–5562.
[20] L. Braunschweiler, R.R. Ernst, *J. Magn. Reson.*, 53 (1993) 521–528.
[21] D.G. Davis, A. Bax, *J. Am. Chem. Soc.*, 107 (1985) 2820–2821.
[22] A. Bax, D.G. Davis, *J. Magn. Reson.*, 65 (1985) 355–360.
[23] U. Piantini, O.W. Sørensen, R.R. Ernst, *J. Am. Chem. Soc.*, 114 (1992) 5449–5451.
[24] A.A. Bothner-By, R.M Stephens, J.-M. Lee, C.D. Warren, R.W. Jeanloz, *J. Am. Chem. Soc.*, 106 (1984) 811–8113.
[25] A. Bax, D.G. Davis, *J. Magn. Reson.*, 63 (1985) 207–213.
[26] M. Guéron, P. Plateu, M. Decorps, *Prog. NMR Spectrosc.*, 23 (1991) 135–209.
[27] M. Piotto, V. Saudek, V. Sklenar, *J. Biomol. NMR*, 2 (1992) 661–666.
[28] D.J. States, R.A. Haberkorn, D.J. Ruben, *J. Magn. Reson.*, 48 (1982) 286–292.
[29] D.V. Renouf, E.F. Hounsell, *Int. J. Biol. Macromol.*, 15 (1993) 37–42.
[30] B. Imperiali, T.L. Hendrickson, *Bioorg. Med. Chem.*, 3 (1995) 1565–1578.
[31] A. Imberty, M.-M. Delage, Y. Bourne, C. Cambillau, S. Perez, *Glycoconjugate J.*, 8 (1991) 9355–9359.
[32] J.T. Davis, S. Hirani, C. Bartlett, B.R. Reid, *J. Biol. Chem.*, 269 (1994) 3331–3338.
[33] J.F.G. Vliegenthart, L. Dorland, H. van Halbeek, *Adv. Carbohydr. Chem. Biochem.*, 41 (1983) 209–374.
[34] M.R. Wormald, W.E. Wooten, R. Bazzo, C.J. Edge, A. Feinstein, T.W. Rademacher, R.A. Dwek, *Eur. J. Biochem.*, 198 (1991) 131–139.
[35] A. Perczel, E. Kollat, M. Hollosi, G.D. Fasman, *Biopolymers*, 33 (1993) 665–683.
[36] J.M. Withka, D.F. Wyss, G. Wagner, A.R. Arlanandam, E.L. Reinherz, M.A. Recny, *Structure*, 1 (1993) 69–81.
[37] H.C. Joao, R.A. Dwek, *Eur. J. Biochem.*, 218 (1993) 239–244.
[38] B. Imperiali, K.W. Rickert, *Proc. Natl. Acad. Sci. USA*, 92 (1995) 97–101.
[39] D.F. Wyss, J.S. Choi, J. Li, M.H. Knoppers, K.J. Willis, A.R.N. Arulanandam, A. Smolyar, E.L. Reinherz, G. Wagner, *Science*, 269 (1995) 1273–1278.
[40] D.H. Live, R.A. Kumar, X. Beebe, S.J. Danishefsky, *Proc. Natl. Acad. Sci. USA*, 93 (1996) 12759–12761.
[41] D.A. Cumming, R.N. Shah, J.J Krepinsky, A.A. Grey, J.P. Carver, *Biochemistry*, 26 (1987) 6655–6663.
[42] P. Wu, K.G. Rice, L. Brand, Y.C. Lee, *Proc. Natl. Acad. Sci. USA*, 88 (1991) 9355–9359.
[43] B. Imperiali, S.E. O'Connor, *Pure Appl. Chem.*, 70 (1998) 33–40.
[44] H. Paulsen, S. Peters, T. Bielfeldt, M. Meldal, K. Bock, *Carbohydr. Res.*, 268 (1993) 17–34.
[45] E. Meinjohanns, M. Meldal, T. Jensen, O. Werdelin, L. Galli-Stampino, S. Mouritsen, K. Bock, *J. Chem. Soc., Perkin Trans. 1*, (1997) 871–884.
[46] N. Mathieux, H. Paulsen, M. Meldal, K. Bock, *J. Chem. Soc., Perkin Trans. 1*, (1997) 2359–2368.
[47] M. Rivière, G. Puzo, *Biochemistry*, 31 (1992) 3575–3580.
[48] R. Liang, A.H. Andreotti, D. Kahne, *J. Am. Chem. Soc.*, 117 (1995) 10395–10396.
[49] I. Matsuo, Y. Nakahara, Y. Ito, T. Nukada, Y. Nakahara, T. Ogawa, *Bioorgan. Med. Chem.*, 3 (1995) 1455–1463.
[50] E. Meinjohanns, M. Meldal, H. Paulsen, R.A. Dwek, K. Bock, *J. Chem. Soc., Perkin Trans. 1*, (1998) 549–561.

[51] T. Patel, J. Bruce, A. Merry, C. Bigge, M. Wormald, A. Jawues, R. Parekh, *Biochemistry*, 32 (1993) 679–693.
[52] J.F.G. Vliegenthart, H. van Halbeek, L. Dorland, *Pure Appl. Chem.*, 53 (1981) 45–77.
[53] B. Imperiali, K.L. Shannon, *Biochemistry*, 30 (1991) 4374–4380.
[54] D.A. Cumming, J.P Carver, *Biochemistry*, 26 (1987) 6664–6676.
[55] R. Boelens, T.M.G. Konig, R. Kaptein, *J. Mol. Struct.*, 173 (1988) 299–311.
[56] B.R. Leeflang, L.M.J. Kroon-Batenburg, *J. Biomol. NMR*, 2 (1995) 495–518.
[57] J.P.M. Lommerse, L.M.J. Kroon-Batenburg, J. Kroon, J.P. Kamerling, J.F.G. Vliegenthart, *J. Biomol. NMR*, 5 (1995) 79–94.
[58] L. Urge, L. Gorbics, L. Otvos Jr., *Biochem. Biophys. Res. Commun.*, 184 (1992) 1125–1132.
[59] P.M. Rudd, R.J. Wood, M.R. Wormald, G. Opdenakker, A.K. Downing, I.D. Campbell, R.A. Dwek, *Biochim. Biophys. Acta*, 1248 (1995) 1–10.
[60] B.A. Spronk, A. Rivera-Sagredo, J.P. Kamerling, J.F.G. Vliegenthart, *Carbohydr. Res.*, 273 (1995) 11–26.
[61] S.W. Homans, R.A. Dwek, D.L. Fernandes, T.W. Rademacher, *FEBS*, 164 (1983) 231–235.
[62] S.W. Homans, R.A. Dwek, T.W. Rademacher, *Biochemistry*, 26 (1987) 6571–6578.
[63] S.W. Homans, R. Pastore, R.A. Dwek, T.W. Rademacher, *Biochemistry*, 26 (1987) 6649–6655.
[64] T. Taguchi, K. Kitajima, Y. Muto, S. Yokoyama, S. Inoue, Y. Inoue, *Eur. J. Biochem.*, 228 (1995) 822–829.